ISSN 1068-3755, Surface Engineering and Applied Electrochemistry, 2015, Vol. 51, No. 4, pp. 313–317. © Allerton Press, Inc., 2015.

Investigation of Solvothermal Synthesis and Formation Mechanism of Fe_2O_3/C Microspheres[1]

H. Safarzadeh, R. Ebrahimi-Kahrizsangi, M. Ghaderi*, and A. Saffar-Talouri

Young Researchers and Elite Club, Najaf Abad Branch, Islamic Azad University, Najaf Abad, Iran

**e-mail: mo.ghaderi@yahoo. com*

Received July 11, 2014; in final form, October 21, 2014

Abstract—In this research we report a one-step method to fabricate Fe_2O_3/C microspheres by using the rolling scales oxides via the solvothermal approach. The thermal gravimetric Analysis (TGA) experiment was carried out in order to determine the amount of carbon in the synthesized samples. Only Fe_2O_3 peaks could be observed from X-ray diffractometry patterns; the carbon in the composite was amorphous. The content of the carbon in the composite was calculated to be about 72 wt %. After annealing at 800°C, scanning electron microscopy images showed that the surface of microspheres was rather smooth and their diameters were in the range of 1–3.5 μm. The investigation of Fe_2O_3/C microspheres formation mechanism revealed that Fe_2O_3 nanoparticles are homogeneously distributed in the carbon matrix.

Keywords: microsphere, solvothermal approach, Fe_2O_3, carbon, electrode

DOI: 10.3103/S1068375515040122

1. INTRODUCTION

Nanostructured transition metal oxides have received great interest as electrodes for lithium-ion batteries [1]. Among these, Fe_2O_3 is an *n*-type, ecofriendly semiconductor that can be used in household and industrial applications for detection of toxic vapors and harmful and flammable gases. This is why, Fe_2O_3 microspheres with a hollow structure are used to make acetone and CO sensors [2]. Also, Fe_2O_3 microspheres are widely used in fabrication of the DNA electrochemical biosensors for determining nucleic acid sequences [3]. The electrodes made of nanooxides of transition metals have a significantly high electrochemical capacity of 700 mAh g^{-1}. Indeed, they can be regarded as promising substitutes for carbon electrodes and Ni-metal hydride in Li-ion batteries [4]. However, the most critical problem that hinders the commercial use is their large specific volume change, resulting in the aggregation of small particles into larger ones [5]. A continuous volume change during charge-discharge results in disintegration of the electrode materials and capacity fading upon cycling [6]. To overcome the volume changes is possible through the use of nano-sized materials and formation of micro composites with carbon, in which the oxide nanoparticles are embedded within the composite. The carbon can act as a barrier to suppress the aggregation of active nano particles and thus increase their structural stability during cycling [7]. The carbon has a high electronic conductivity, and it can improve the conductance of the active materials and the electrochemical capacity of nano-oxides.

In order to produce microcomposites of metal oxides with carbon, several methods, including molten salt process [8], two-step synthesis by graphene [9], hydroxide and hydrothermal routes [10], flocculation [11], sol-gel [12], and spray pyrolysis [13], have been suggested.

The present research aims at using the rolling scales oxide wastes that have not found much application so far in a one-step production of Fe_2O_3/C composite microspheres by the solvothermal method.

2. MATERIALS AND METHODOLOGY

The most important materials used in this research were: 2.5 g of oxide shells with 97 wt % iron oxide purity, 160 mL ethanol (96%), 50 mL sulfuric acid 99%, 2 g glucose 100%, 5 mL nitric acid 65%, and 2 g sodium hydroxide.

First, oxide shells were dissolved in a concentrated sulfuric acid. Then the solution was exposed to sever magnetic stirring at 100°C for 30 min. Following that, nitric acid was slowly added to the solution. This resulted in a complete solution of all oxide solid particles. Then the solution was heated until it was entirely dried. The white precipitate at the bottom largely contained Fe^{+3} [14].

Next, 2.5 g of Fe^{+3} were mixed with 160 mL of ethanol and thoroughly stirred with a magnetic stirrer. The solution was heated up to 60°C until all the iron salt was solved. Due to the solving of the iron salt, the

[1] The article is published in the original.

Elearnica Downloaded from http://www.elearnica.ir

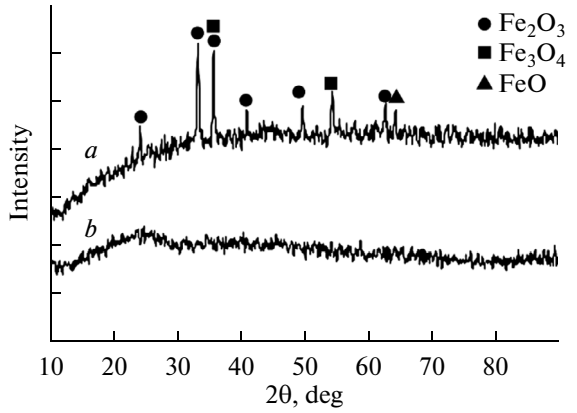

Fig. 1. XRD pattern of Fe_2O_3/C microspheres in two conditions: (*a*) without being annealed; (*b*) annealed.

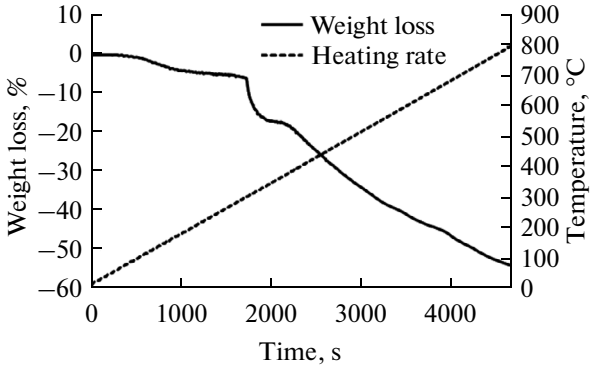

Fig. 2. Thermogravimetric curve of amorphous Fe_2O_3/C powder samples resulting from solvothermal reaction in the range from room temperature to 800°C.

solution pH decreased to 1.7. In the next stage, 2 g of glucose were solved in 5 mL deionized water and then added to the above solution. The solution was transferred to an autoclave and stored at 185°C for 25 h and then air-cooled to room temperature. The resulting black precipitates were washed several times with ethanol and centrifuged. This caused the separation of all anions and cations from the precipitates. The as-prepared precipitates were designated amorphous Fe_2O_3/C hybrid microspheres. The products were finally dried in an oven at 50°C for 10 h.

The amorphous Fe_2O_3/C samples obtained via the solvothermal reaction were annealed in the tube furnace at 800°C in an argon-rich atmosphere.

The composite properties such as crystallite or amorphous structure, crystallinity degree, and grain size were investigated by a Philips X'pert high score X-ray difractometer with CuK_α radiation (2θ is chosen in the range of 10°–90°. Thermogravimetric analysis was performed on a TGA 401 instrument at up to 800°C and the heating rate of 10°C min^{-1} in air. The microstructure of the as-prepared composite was observed with the scanning electron microscope (LEO-VP435).

3. RESULTS AND DISCUSSION

3.1. Characterization of Fe_2O_3/C Microspheres

Figure 1 shows X-ray diffraction (XRD) patterns of amorphous and annealed Fe_2O_3/C microspheres. As can be seen in Fig. 1, *a*, Fe_2O_3/C microspheres are amorphous. Heating in argon atmosphere at 800°C caused significant crystallization of Fe_2O_3/C samples (Fig. 1, *b*). The peaks of the annealed sample are located in 33.2, 35.7, 40.8, 54.2, 62.4, and 64.2 angles which are assigned as (104), (110), (113), (024), (116), (214), and (300) reflections, respectively. The carbon is amorphous in both conditions which is similar to the results reported by Qiao [15]. The intensity of some peaks is weak due to the presence of impurities in the composite. Also, during the annealing process some amount of Fe_2O_3 changed into Fe_3O_4 because of a high temperature and the carbon presence. The Fe_2O_3 grain size was calculated based on the modified Debye Scherrer's equation (Eq. 1):

$$L = 0.89\lambda/\beta\cos\theta$$
$$\beta = \frac{k\lambda}{L\cos\theta} \Rightarrow \ln\beta = \ln\frac{k\lambda}{L} + \ln\frac{1}{\cos\theta}. \quad (1)$$

By plotting lnβ variations against ln(1/cosθ) the intercept of a least squares line regression, ln = $K\lambda/L$, is obtained. After the calculations of the phase analysis (XRD) results of Fe_2O_3/C powder, the obtained y-intercept was −5.4886. Since λ = 1.54059 Å and K = 0.89, the Fe_2O_3 nanoparticles size (L) was averagely calculated as 30 ± 4 nm.

Figure 2 shows the weight variations diagram for amorphous Fe_2O_3/C powder samples resulting from solvothermal reaction. Thermogravimetric curve shows that the weight loss occurs in three stages. The first stage takes place in the temperature range of 100 to 330°C. The weight loss at this stage is estimated to 5.8%, which can be due to the evaporation and removal of water from the composite [5].

The second stage happens in the temperature range of 330 to 360°C and the weight loss is calculated to be 12.2%. The main reason of the weight loss at this stage is that iron hydroxide changes into iron oxide along with the formation of vapor during the process (Eqs. 2 and 3).

$$2Fe(OH)_3 \rightarrow Fe_2O_3 + 3H_2O, \quad (2)$$

$$C_6H_{12}O_6 \rightarrow 6C + 6H_2O. \quad (3)$$

The third stage, from 360 to 800°C, is related to oxidation of the amorphous carbon. The weight loss in this stage is 36% [16]. Based on the calculations from thermos-gravimetric curve and complete carbon oxidation, the carbon content in the composite was estimated to be 72%.

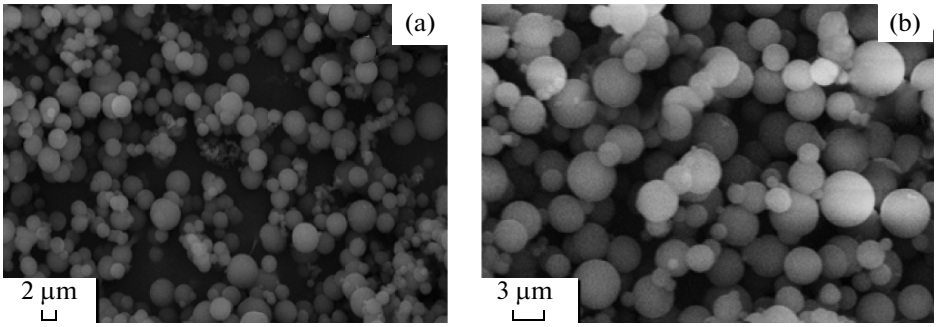

Fig. 3. SEM image of Fe_2O_3/C microspheres in which Fe_2O_3 nanoparticles (30 ± 4 nm) are distributed in the carbon spheres: (a) in amorphous condition; (b) annealed at 800°C.

Figure 3a shows the spherical morphology of the composites as taken from the surface of Fe_2O_3/C microspheres. Their sizes are almost uniform and their diameters are in the range 1–3.5 μm. Figure 3b shows the image of Fe_2O_3/C microspheres with higher magnification after annealing. The size and shape of the microspheres have remained the same after annealing, but the surfaces have become slightly rough due to gas emission. It has been proved that Fe_2O_3 nanoparticles are homogeneously distributed in the carbon matrix [5].

Results revealed that Fe_2O_3/C microspheres could not be obtained via the solvothermal treatment below 140°C, which is in agreement with the reports by other researchers [16]. In the absence of the iron salt precursor no product is obtained from glucose and ethanol. Also, in order to achieve a spherical morphology the solution pH should be less than 2 [16]. Figure 4 shows SEM image of the sample in which the pH value went up to 2.5 because of the addition of adding sodium hydroxide. As can be seen, the morphology tends toward aggregation.

3.2. Fe_2O_3/C Microspheres Formation Mechanism

The mechanism of Fe_2O_3/C microspheres formation comprises two stages, namely nucleation and growth. The initial nucleus shape is inherent and depends on the innate properties of the composite. In contrast, the growth stage is a thermodynamic and controllable factor [17]. The mechanism of formation includes production of aromatic primary compounds containing cations and polymerization of glucose. After that, the carbon and metal oxide nanoparticles are produced simultaneously and metal oxide nanoparticles are distributed in the carbon matrix. In glucose polymerization, hydrophobic groups play the role of tails and include radical combinations of hydrocarbon (C–H). The hydrophilic head includes OH-, CHO-, and COO-groups [16, 18]. Fe^{+3} cations are attracted by hydrophilic spherical micelle parts due to electrostatic processes [19]. Glucose influences the surface tension of ethanol and can dramatically govern the nucleation rate of Fe_2O_3 particles. When the Fe_2O_3 nucleation rate increases, smaller particles with nanometer sizes are formed [19]. Following that, by glucose polymerization, the concentration reaches the critical micelle concentration and a spherical micelle complex, with hydrophobic groups as the micelle core and the hydrophilic hydroxyls as the outer surface of micelle core are formed. Figure 5 shows how Fe_2O_3/C microspheres are formed. After nucleation, the hydrophilic hydroxyls are still anchored to the closest free molecules [18], which causes the watering of the nucleus and hence the micelle growth. Fe^{+3} cations are continuously attracted by the hydrophilic parts of the growing sphere and change into Fe_2O_3 after $Fe(OH)_3$ is formed. This trend continues until all glucose molecules are consumed.

The spherical appearance of the as-synthesized microcomposites can be explained in this way: chemical reactions generally move in a certain direction, which results in the decrease of the Gibbs free energy. Formation of microspheres must be related to the Gibbs free energy. On the other hand, the molecules surface stresses should reach a minimum by formation of spherical morphology, so as to reduce the surface free energy. In fact, in the formation of the final com-

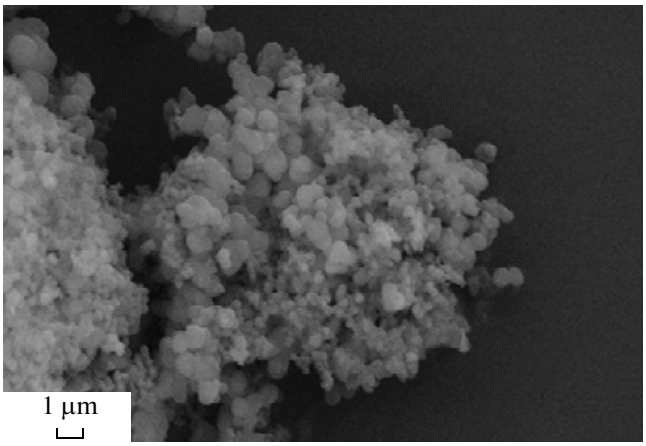

Fig. 4. SEM image of a sample with pH = 2.5.

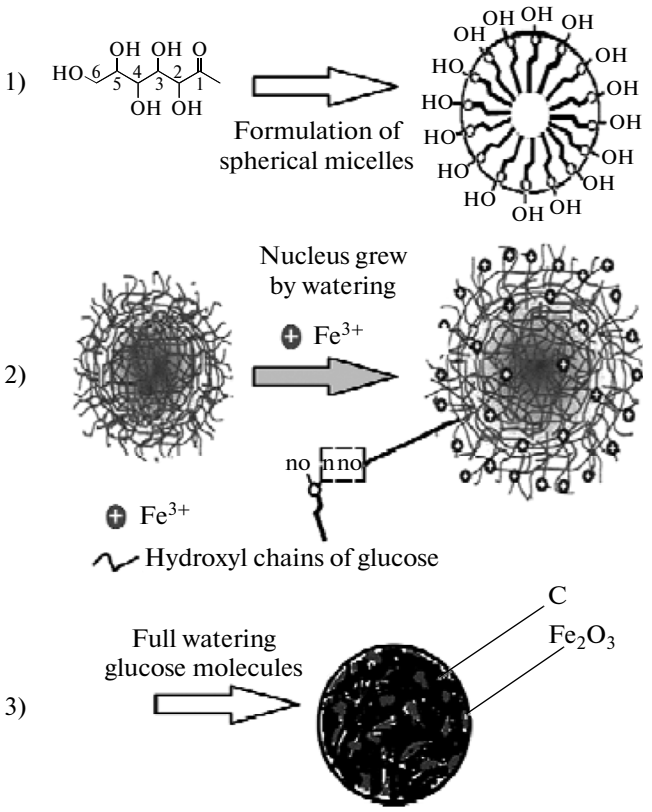

Fig. 5. Schematic illustration of formation of initial nuclei of Fe_2O_3/C microspheres and nucleus growth.

posite shape there is a competition between the surface free energy and the Gibbs free energy. When the particle size is small, the surface free energy is the dominant mechanism and with formation of the spherical morphology reaches a minimum value due to the lowest surface to volume ratio [20].

Gradually, with the increase of the spheres size, the surface free energy plays a less significant role in the material morphology. However, it should be noted that with control of variable such as temperature, precursor concentration, pH, and the like we can make variations as to the role played by either the Gibbs free energy or the surface free energy.

4. CONCLUSIONS

In this research, microspherical Fe_2O_3/C composites were prepared via the solvothermal approach by using the mill scale oxide shells and the following results were obtained:

(1) XRD patterns quite evidently depicted Fe_2O_3 peaks. Also, by studying the growth mechanism, it can be inferred that Fe_2O_3 nanoparticles are homogeneously distributed in the carbon matrix. The carbon content in the composite is amorphous in both annealed and un-annealed conditions.

(2) Based on the thermos-gravimetric curve and complete carbon oxidation, the carbon content in microspherical Fe_2O_3/C composites was estimated to be 72%.

(3) SEM images revealed a spherical and smooth morphology. The sizes of the microspheres were rather uniform and their diameters were in the range of 1–3.5 μm.

(4) For synthesis of Fe_2O_3/C microspheres the solution pH should be lower than 2 and the temperature should be above 140°C.

(5) In addition to providing carbon, glucose decreases the surface tension of ethanol and increases the nucleation rate of Fe_2O_3 nanoparticles, thus decreasing the grain size of Fe_2O_3 particles near the hydrophobic chain.

REFERENCES

1. Poizot, P., Laruelle, S., Grugeon, S., Dupont, L., and Tarascon, J.M., Towards the next generation of Li-ion batteries based on nanomaterials, *Nature,* 2000, vol. 407, pp. 496–499.
2. Wang, S.L., Wang, T., Yang, X., Liu, H., Zhang, J., Zhu, B., and Zhang, S., Porous a-Fe_2O_3 hollow microspheres and their application for acetone sensor, *J. Solid. State Chem.*, 2000, vol. 183, pp. 2869–2876.
3. Zhang, W., Yang, T., Li, X., Wang, D., and Jiao, K., Conductive architecture of Fe_2O_3 microspheres/self-doped polyaniline nanofibers on carbon ionic liquid electrode for impedance sensing of DNA hybridization, *Biosens. Bioelectron.*, 2009, vol. 25, pp. 428–434.
4. Anandan, K. and Rajendran, V., Morphological and size effects of NiO nanoparticles via solvothermal process and their optical properties, *Mat. Sci. Semicon. Proc.*, 2011, vol. 14, pp. 43–47.
5. Qiao, H., Luo, Q., Fu, J., Li, J., and Kumar, D., Solvothermal preparation and lithium storage properties of Fe_2O_3/C hybrid microspheres, *J. Alloy Compd.*, 2012, vol. 513, pp. 220–223.
6. Huang, X.H., Wang, C.B., Zhang, S.Y., and Zhou, F., CuO/C microspheres as anode materials for lithium ion batteries, *Electrochim Acta*, 2011, vol. 56, pp. 6752–6756.
7. Qiao, H., Yao, D., Cai, Y., Huang, F., and Wei, Q., One-pot synthesis and electrochemical property of MnO/C hybrid microspheres, *Ionics*, 2013, vol. 19, pp. 595–600.
8. Hassan, M.F., Rahman, M.M., Guo, Z.P., Chen, Z.X., and Liu, H.K., Solvent-assisted molten salt process: A new route to synthesise Fe_2O_3/C nanocomposite and its electrochemical performance in lithium-ion batteries, *Electrochim Acta*, 2010, vol. 55, pp. 5006–5013.
9. Liu, S.Y., Xie, J., Pan, Q., Wu, C.Y., Cao, G.S., Zhu, T., and Zhao, X.B., Graphene anchored with nanocrystal Fe_2O_3 with improved electrochemical li-storage properties, *Int. J. Electrochemical. Science*, 2012, vol. 7, pp. 354–362.
10. Huang, X.H., Tu, J.P., Zhang, C.Q., and Xiang, J.Y., Net-structured NiO-C nano composite as Li-interca-

lation electrode material, *Electrochem. Commun.,* 2007, vol. 9, pp. 1180–1184.

11. Mi, H., Xu, Y., Shi, W., Yoo, H., and Mo Oh, S., Flocculant-assisted synthesis of Fe_2O_3/carbon composites for superior lithium rechargeable batteries, *Mater. Res. Bull.,* 2012, vol. 47, pp. 152–155.
12. Li, M.Y., Wang, Y., Liu, C.L., Gao, H., and Dong, W.S., Iron oxide/carbon microsphere lithium-ion battery electrode with high capacity and good cycling stability, *Electrochim Acta*, 2012, vol. 67, pp. 187–193.
13. Rahman, M.M., Chou, S.L., Zhong, C., Wang, J.Z., Wexler, D., and Liu, H.K., Spray pyrolyzed NiO–C nanocomposite as an anode material for the lithium-ion battery with enhanced capacity retention, *Solid State Ionics*, 2012, vol. 180, pp. 1646–1651.
14. Legodi, M.A. and Waal, D.D., The preparation of magnetite, goethite, hematite and maghemite of pigment quality from mill scale iron waste, *Dyes Pigments*, 2007, vol. 74, pp. 161–168.
15. Qiao, H., Xiao, L., Zheng, Z., Liu, H., Jia, F., and Zhang, L., One-pot synthesis of CoO/C hybrid microspheres as anode materials for lithium-ion batteries, *J. Power Sources*, 2008, vol. 185, pp. 486–491.
16. Zheng, J. and Liu, Z.Q., One-step solvothermal synthesis of Fe_3O_4/C core-shell nanoparticles with tunable sizes, *Nanotechnology*, 2012, vol. 23, p. 165601.
17. Wang, L., Zhao, Y., Lai, Q., and Hao, Y., Preparation of 3D rose-like NiO complex structure and its electrochemical property, *J. Alloy Compd.,* 2010, vol. 95, pp. 82–87.
18. Wang, Q., Li, H., Chen, L., and Huang, X., Novel spherical microporous carbon as anode material for Li-ion batteries, *Solid State Ionics,* 2002, vol. 152, pp. 43–50.
19. Du, H., Jiao, L., Wang, Q., Guo, L., Wang, Y., and Yuan, H., Facile carbonaceous microspheres templated synthesis of Co_3O_4 hollow spheres and their electrochemical performances in supercapacitors, *Nano Research*, 2013, vol. 6, pp. 87–98.
20. Chen, Y., Shi, X., Han, B., Qin, H., Li, Z., and Lu, Y., The complete control for the nanosize of spherical MCM-41, *JNN*, 2012, vol. 12, pp. 1–11.